Soil liquefaction assessment of Ecuadorian coastal region using SDMT test (Puerto Baquerizo site)

Christian Ramirez[1], *Freddy* Arias[1], *Davide* Besenzon[1], *Sara* Amoroso[2,3], *Kerwin* Chunga[4]

[1]*University Superior Polytechnical Del Litoral (ESPOL), Department of Earth Sciences, Guayaquil, Ecuador,* chracarv@espol.edu.ec, fdarias@espol.com.ec, besenzon@espol.edu.ec

[2]*University of Chieti-Pescara, Department of Engineering and Geology, Pescara, Italy,*
[3]*Istituto Nazionale di Geofisica e Vulcanologia, L'Aquila, Italy,*
sara.amoroso@unich.it

[4]*Universidad Técnica de Manabí, Departamento de Construcciones civiles, Portoviejo, Ecuador,*
kervin.chunga@utm.edu.ec

ABSTRACT

On March 18, 2023, a Mw6.6 earthquake hit the South Guayas coastal region (Ecuador), resulting in human fatalities and extensive structural damage. The event triggered widespread soil liquefaction evidences by significant volume of ejected material, which persisted several weeks following the event, marking the epicentral area prone to liquefaction. To assess the susceptibility to seismic-induced soil liquefaction, we performed one seismic dilatometer test (SDMT) in an area where the phenomenon clearly manifested. This study aims to evaluate and compare various established SDMT methods for predicting soil liquefaction potential under the specific 2023 seismic event. The findings are expected to enhance the understanding of liquefaction and contribute to improve seismic hazard assessment in areas along the Ecuadorian coast, which are often interested by earthquakes, as well as to the development of mitigation strategies in this earthquake prone coastal region.

Keywords: soil liquefaction, seismic dilatometer test, horizontal stress index, shear wave velocity

1. Introduction

The evaluation of the liquefaction potential in sandy soils has traditionally been carried out by approximating the cyclic resistance of the material using empirical correlations with field test results, and comparing them with the shear stress levels that are expected to be induced by a specific seismic event (Kishida 1966, Zhou 1980, Youd et al. 2001, Cetin et al. 2004, Moss et al. 2006, Idriss and Boulanger 2008, Boulanger and Idriss 2014). The use of these tests is justified by the correlation between some geotechnical properties linked to liquefaction potential (relative density, lateral stress, cementation, age, stress history) and parameters measured in the tests (cone tip resistance, blow count, etc.), as reported by Idriss and Boulanger, (2008).

The use of the flat dilatometer test (DMT) for the evaluation of the liquefaction potential was proposed taking advantage of the relationship between the horizontal stress index (K_D) with some geotechnical properties closely linked to the liquefaction phenomenon (relative density D_R, in situ earth pressure coefficient K_0, overconsolidation ratio OCR, aging, cementation, state parameter; Marchetti 1982, Robertson and Campanella 1986, Reyna and Chameau 1991, Yu 2004, Monaco et al. 2005).

The addition of the seismic modulus in the DMT equipment (converting it into SDMT) also allows the evaluation of the cyclic resistance from the shear wave velocity of the material (V_S; Marchetti et al. 2008), converting the SDMT into a test with great versatility for the evaluation of the liquefaction potential in sandy soils.

Following the 2016 Mw7.8 Ecuador earthquake, the induced liquefaction triggered in Manabi area were well-documented with observations and in situ test results (Ortiz-Hernandez et al. 2022, Salocchi et al. 2020, Vera et al. 2019). Most of the case histories were developed using standard penetration test (SPT) and piezocone test (CPTu) data, while limited research was available from other in situ tests, such as dynamic penetration test with Chinese hammer (DPT) and seismic dilatometer test (SDMT). This paper introduces the liquefaction potential assessment of cohesionless soils in Puerto Baquerizo (Coastal area of Ecuador) through methodologies based on the use of SDMT and its correlation with the levels of liquefaction damage observed after the Balao earthquake Mw6.6.

2. Earthquake-induced soil liquefaction after Balao earthquake

As a consequence of the Mw6.6 earthquake, soil liquefaction was triggered in several points in the southern Ecuador. The clearest evidence of this phenomenon was observed in places between 10 and 50 km away from the epicenter of the event. The earthquake-induced soil liquefaction was related to several damages and structural collapses, especially in urban areas such as Machala and Puerto Bolívar (South Guayas and El Oro coastal regions).

Particularly in Puerto Baquerizo (Fig. 1), 35 km far from the epicenter, the liquefaction was evidenced by the widespread presence of sand boils with radius from 0.20 m to 1.50 m, sand ejecta to the surface, and presence of ground cracks between 4 and 6 cm wide. Since Puerto Baquerizo is essentially a rural area, the structures built in this zone are mainly composed of low-rise concrete or composite (wood and concrete) residences. Therefore, no structural collapse was reported. However, damage to foundation beams, cracking of masonry and floors were observed in buildings near the points where the liquefaction was triggered. No information was found regarding the topography of Puerto Baquerizo prior to the earthquake, but the observed damage and distortion in some structural elements indicated the occurrence of important volumetric and differential settlements.

3. Liquefaction assessment for Puerto Baquerizo site using SDMT data

3.1. Geological setting of Puerto Baquerizo

According to the geological map of Ecuador published by the Ecuadorian Institute of Geological, Mining and Metallurgical Research (Eguez, Gaona and Albán 2017), Puerto Baquerizo is located in a transition zone between Holocene alluvial deposits of the west of the Andes, underlaying Quaternary marine terraces in estuarine regions of the central-southern Ecuador (Fig. 2).

The Holocene alluvial deposits of the Ecuadorian coast are composed of intercalations of silt, clay and fine sand, while the marine terraces are mainly composed of soft marine clay deposits.

3.2. Site investigation program

The SDMT test was carried out where the liquefaction effects were clearly observed, close to the sand volcanoes shown in Fig 1. The corrected lift off (p_0) and 1.1 mm deformation pressures (p_1) were measured every 0.2 m up to 20 m depth, while the equilibrium pressure after deflation (p_2) was carried out at levels where the presence of materials with drained behavior was hypothesized. In these conditions the p_2 tends to be equal to the hydrostatic pressure. Observing the variation of the p_2 readings with depth, the ground water table was located 1.8 m from the surface. The shear wave velocity (V_S) measurements were carried out each 0.5 m above 8 m depth, and each 1.0 m between 8 m and 17 m.

According to the interpretation of the SDMT results, between the surface and 2.6 m depth there is a layer of cohesive material named for this study “shallow clay” (Fig. 3). The material index (I_D) ranges between 0.1 and 0.5, while horizontal stress index (K_D) decreases from 5 to 2.1 between the beginning of the test and the lower boundary of the stratum. The shear wave velocity varies between 80 and 100 m/s.

Underlaying the “shallow clay” to 6.5 m of depth, “silty sand” deposits were identified (Fig. 3). The material index was slightly ranging between 1.70 and 2.10. Horizontal stress index (K_D) shows a significant increase between 4.5 m and 6 m depth, reaching magnitudes between 6 and 7.5. At the upper and lower boundaries of the stratum the K_D values tend to be in the range between 3 and 4. The V_S measured in this layer are between 110 and 160 m/s. As already observed for K_D, the shear wave velocities also show a maximum value around the same depth interval (4.5 and 6 m).

Figure 1. Ground Cracking, sand boils and ejected soil as a liquefaction evidence in Puerto Baquerizo.

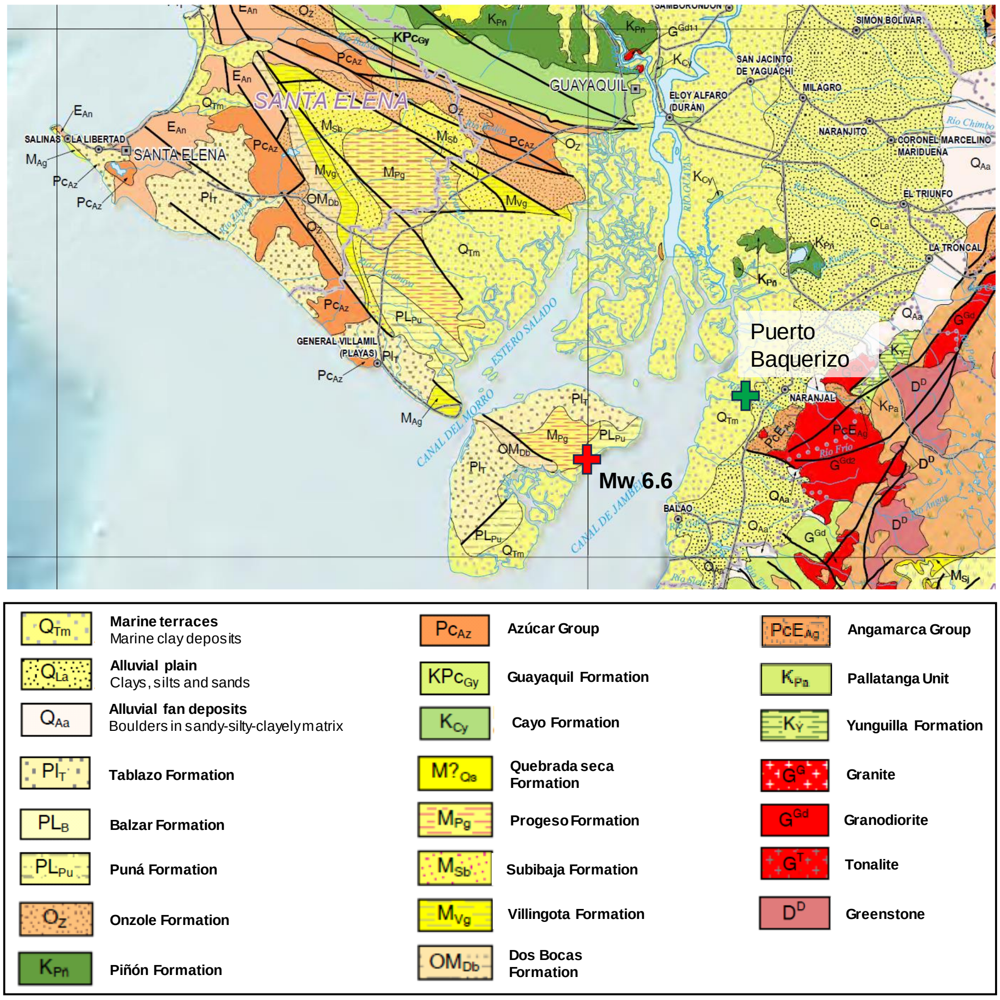

Figure 2. Geological setting of Ecuadorian Central Coastal Area (Eguez, Gaona and Albán 2017). Recovered from https://www.geoenergia.gob.ec/mapas-geologicos/

Successive intercalations of thin layers of cohesive materials (clays or silts) and silty sands to sandy silts were observed between 6.5 m and 16.5 m depth, since I_D varies widely with depth, ranging between 0.05 and 1.20. Since it is complex to determine if one of the two types of materials predominates over the other, it was decided to group this succession of layers into a single stratum called "silty sand/silty clay mixture" (Fig. 3). However, the K_D shows small variations throughout the stratum, typically being between 2 and 3.5, although, at certain levels K_D greater than 4 were determined. The measured shear wave velocities increased gradually with depth between 10 and 15 m, moving from 100 m/s to 180 m/s.

Below 16.5 m until the end of the test (20 m), the soil was classified completely as clay, according to the I_D. For this study, the layer was called "deep clay" (Fig. 3). In correspondence at these depths, K_D values between 3.5 and 3.7 were determined. The measured shear wave velocities decreased to 100 m/s.

Considering the relationship between the liquefaction expressions observed on the surface with (i) the thickness of the liquefiable layer, and (ii) the presence or absence of non-liquefiable layers above the liquefiable material and their thickness, it is presumed that the source of liquefaction and its effects is the "silty sand" layer, both because of its proximity to the surface and its thickness (approximately 3.9 m). This statement will be discussed in greater detail later.

3.3. Ground motion estimation

One of the most important issues in the development of the present assessment was the estimation of the seismic intensity in Puerto Baquerizo during the Mw6.6 earthquake. Only through this estimation it is possible to approximate with an appropriate degree of confidence the shear stresses that were induced in the ground.

According to data published by the Geophysics Institute of the National Polytechnical University (IGEPN, https://www.igepn.edu.ec) and measured by the Ecuadorian Accelerograph Network (RENAC), the effects of the earthquake were recorded by at least eight stations located at distances between 49 km and 157 km from the epicenter of the event. These stations are located in cities of the Center-South of Ecuador, such as: Guayaquil, Arenillas, Cuenca, Machala and Loja. The peak ground accelerations (PGAs) reported by RENAC vary between 0.32 g (station ACH1, located in Machala, 54 km from the epicenter) and 0.05 g (station ALJ1, located in Loja, 157 km from the epicenter).

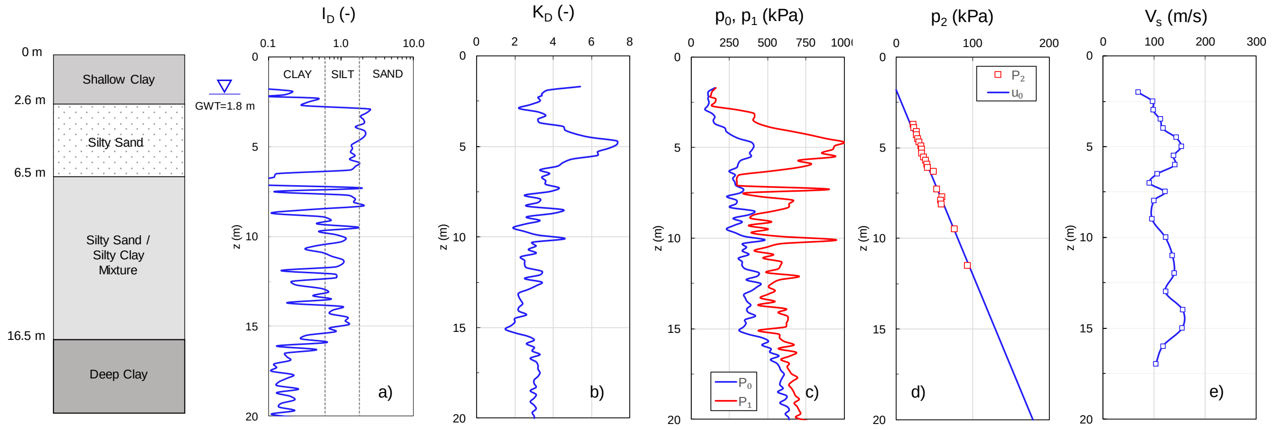

Figure 3. Variation with depth: a) Material index (I_D); b) Horizontal stress index (K_D); c) corrected lift off pressure (p_0) and 1.1 mm deflection pressure (p_1); d) corrected equilibrium pressure after deflating (p_2) and hydrostatic pore water pressure (u_0); and e) shear wave velocity (V_s).

No official information regarding the specific geotechnical conditions of the sites where the accelerographs are installed was found. However, from an analysis of the measured PGAs it can be deduced that site effects could have occurred in stations such as ACH1 (Machala) and GYKA (South of Guayaquil) since the intensity levels are substantially higher than those recorded in other stations that were found at similar epicentral distances (ACH2 and AC07). Furthermore, added to this possible site effect, it is likely that a directivity effect occurred in the earthquake towards the South of the Equator. This would explain the record of higher levels of seismic intensity towards the South of the event, especially at the Machala and Arenillas stations.

The seismic intensity estimation in Puerto Baquerizo was carried out by applying Ground Motion Prediction Equations (GMPEs) proposed by different authors for in-slab earthquakes. This decision was made since the RENAC stations closest to the study site are between 60 and 70 km away, and with slightly greater epicentral distances. Therefore, their measurements were not considered representative of the accelerations induced in Puerto Baquerizo. However, by having both the epicentral distance and the recorded PGA well documented, the information provided by the RENAC represented an important database for the validation of the predictions made by the GMPEs.

The models selected for the evaluation were: Youngs et al. (1997), Atkinson and Boore (2003) and Zhao et al. (2006). The GMPEs proposed by Atkinson and Boore (2003) and Zhao et al. (2006) include site factors to evaluate the effect of the dynamic properties of the deposit on the expected seismic intensities. The selection of the site factors was carried out considering the classification proposed by each author and the shear wave velocities measured by the SDMT. In both cases, the chosen site parameters correspond to the most unfavorable ground condition, which meant, NEHRP E or NEHRP F type soils, with average shear-wave velocity for the upper 30 m depth (V_{30}) less than 200 m/s.

The epicentral distance to Puerto Baquerizo site is approximately 35 km. For this distance the models predict accelerations between 274 cm/s^2 (0.28g) and 470 cm/s^2 (0.48g), in agreement to the models of Youngs et al. (1997) and Zhao et al. (2006), respectively. Finally, the Atkinson and Boore (2003) equation determined a PGA of 372 cm/s^2 (0.38g). For the liquefaction potential analysis, the geometric mean of the three calculated accelerations was used, which means, 343 cm/s^2 (0.35g).

3.4. Cyclic resistance ratio estimation

The cyclic resistance ratio from the horizontal stress index (K_D) was estimated from five correlations, which are detailed below in Eq.1 to Eq. 5.

- Monaco et al. (2000):

$$CRR_{7.5} = 0.0107K_D^3 - 0.0741K_D^2 + 0.2169K_D - 0.1306 \quad (1)$$

- Tsai et al. (2009):

$$CRR_{7.5} = exp\left[\left(\frac{K_D}{8.8}\right)^3 - \left(\frac{K_D}{6.5}\right)^2 + \left(\frac{K_D}{2.5}\right) - 3.1\right] \quad (2)$$

- Robertson (2012):

$$CRR_{7.5} = 93(0.025K_D)^3 + 0.08 \quad (3)$$

- Marchetti (2016):

$$CRR_{7.5} = exp\left[\left(\frac{Q_{cn}}{540}\right) + \left(\frac{Q_{cn}}{67}\right)^2 - \left(\frac{Q_{cn}}{80}\right)^3 + \left(\frac{Q_{cn}}{114}\right)^4 - 3\right] \quad (4a)$$

with

$$Q_{cn} = 25K_D \quad (4b)$$

- Chiaradonna and Monaco (2022):

$$CRR_{7.5} = \exp\,(0.0011097K_D^4 - 0.00569K_D^3 + 0.000625K_D^2 + 0.221K_D - 2.8) \quad (5)$$

To differentiate between cohesionless soils and cohesive soils, the material index (I_D) was used as a criterion. The SDMT data were filtered to only calculate the CRR in soils where I_D was greater than 1.2, associated to the boundary between silts and sandy silt according to Marchetti and Crapps (1981).

On the other hand, two V_S-based methods were selected to determine the CRR of cohesionless materials, Andrus and Stokoe (2000) and Kayen et al. (2013). The correlations proposed by the authors are detailed in the Eq. 6 and Eq. 7.

- Andrus and Stokoe (2000):

$$CRR_{7.5} = \left[0.022\left(\frac{V_{s1}}{100}\right)^2 + 2.8\left(\frac{1}{V_{s1}^* - V_{s1}} - \frac{1}{V_{s1}^*}\right)\right] \quad (6)$$

with

$$V_{s1} = C_v V_s \quad (6a)$$

$$C_v = \left(\frac{P_a}{\sigma'_{vo}}\right)^{0.25} \quad (6b)$$

$$V_{s1}^* = 215 \text{ m/s for FC} \leq 5\% \quad (6c)$$

$$V_{s1}^* = 200 \text{ m/s for FC} \geq 35\,\% \quad (6d)$$

$$V_{s1}^* = \text{varies linearly from 215 m/s to 200 m/s for } 5\% \leq \text{FC} \leq 35\,\% \quad (6e)$$

- Kayen et al. (2013):

$$CRR_{7.5} = exp\{[(0.0073V_{s1})^{2.8011} - 2.6168\ln(M_w) - 0.0099\ln(\sigma'_{vo}) + 0.0028FC - 0.4809\Phi^{-1}(P_L)]/1.946\} \quad (7)$$

For the Kayen et al. (2013) model V_{s1} is also defined by Eq. 6a and Eq. 6b. The term Mw represent the moment magnitude of the event (Mw6.6 for this case history). Also, Kayen et al (2013) include a probabilistic term, which is the inverse cumulative normal distribution $\Phi^{-1}(P_L)$. This term was defined to a liquefaction probability (P_L) of 15%.

The effective vertical stress (σ'_{vo}) was computed assuming a ground water table at 1.0 m depth rather the 1.8 m depth (detected in SDMT test), in both cases Andrus and Stokoe (2000) and Kayen et al. (2013). This assumption takes into account that March (when the earthquake occurred) is part of the rainy season in the Coast of Ecuador, and the test was performed in months where low levels of precipitations exist in the area.

Both V_S-based methods include cyclic resistance adjustment terms for fines content (FC). This measurement is not directly provided by the SDMT results, but it is usually a complementary information carried out from boreholes and related laboratory analysis of recovered samples. An estimation of the fines content (FC) was made through I_D using the proposed correlation by Di Buccio et al. (2023). The FC resulting from this evaluation was used both as a differentiation criterion between soils with cohesive or cohesionless behaviour, as well as for the calculation of the $CRR_{7.5}$ from Andrus and Stokoe (2000) and Kayen et al. (2013).

3.5. Cyclic stress ratio estimation

The cyclic stress ratio corrected for a Mw7.5 ($CSR_{7.5}$) was determined by applying the simplified procedure proposed by Seed and Idriss (1971), both for the K_D-based methods and for V_S-based methods. This model indicates that the $CSR_{7.5}$ is determined from the following expression:

$$\text{CSR}_{7.5} = 0.65 * \left(\frac{a_{max}}{g}\right) * r_d * \left(\frac{\sigma_{vo}}{\sigma'_{vo}}\right) * \frac{1}{\text{MSF}} \quad (8)$$

In the Seed and Idriss (1971) model (Eq. 8) the term "a_{max}" represents the maximum horizontal acceleration at surface and "g" correspond to the gravity acceleration. For this study purposes, a_{max} was considered equal to the peak ground acceleration (PGA) computed using the RENAC data and GMPEs evaluation, which meant, 343 cm/s^2.

According to selection of the ground water table for the $CRR_{7.5}$ evaluation, a ground water table at 1.0 m depth was also selected for the calculation of the effective vertical stress (σ'_{vo}) and total vertical stress (σ_{vo}) .

The stress reduction coefficient (r_d) and the magnitude scale factor (MSF) were determined from the formulations proposed by Idriss and Boulanger (2008), for the liquefaction assessment using K_D-based on methods.

Andrus and Stokoe (2000) synthesized their method using the stress reduction coefficient (r_d) and magnitude scale factor (MSF) relationships recommended by the NCEER Workshop (Youd et al. 2001). To be consistent with the considerations made by the author, the same relationships of the NCEER Workshop model (Youd et al. 2001) were used for the calculation of the seismic demand in the evaluation of the liquefaction potential based on the Andrus and Stokoe method (2000).

For the Kayen et al. (2013) method, the specific relationships proposed by the author were used to calculate the stress reduction coefficient (r_d) and the magnitude scale factor (named DWF in Kayen et al. 2013).

4. Results and discussions

The cyclic stress ratio ($CSR_{7.5}$) was estimated between 0.31 and 0.34 in the "silty sand" (black dots in Fig. 4) and "silty sand / silty clay mixture" (white dots in Fig. 4) layers from Idriss and Boulanger (2008). This approximation coincides with the demands calculated through the model proposed by Youd et al. (2001). However, using the model proposed by Kayen et al. (2013), the cyclic stress ratio estimated for the same layers were about 0.20 and 0.29 (red dots in Fig. 4). This represents between 64% and 88% the cyclic stress ratio determined through Idriss and Boulanger (2008) and Youd et al. (2001).

The cyclic resistance ratios estimated for materials with K_D from 2 to 4 were ranging between 0.10 and 0.20, being Monaco et al. (2005) and Marchetti (2016) the correlations which gives the highest and lowest cyclic resistances for materials with K_D from 2 to 4, respectively (Fig. 4). This represents safety factors against liquefaction of the order of 0.3 and 0.7 for both "silty sand" and "silty sand / silty clay mixtures" layers.

However, it is important to note the difference in the resistances calculated by the methods for K_D greater than 4. Especially the limit value of K_D above which liquefaction is no longer expected to occur. For example, from Monaco et al. (2005) liquefaction is not expected in materials with K_D greater than 4.3. This K_D "limit" is considerably larger if the cyclic resistance is evaluated using the correlations of Tsai et al. (2009) and Marchetti (2016), which are the ones that report the most conservative resistances.

In the particular case of Puerto Baquerizo, the major part of cohesionless soils were classified as silty sands or sandy silts with K_D less than 4.5. Therefore, according to the results obtained, they are defined as liquefiable in almost all cases. However, in the "silty sand" layer there are some materials (between 4.5 m and 6.0 m, around 38% of the source layer) where the calculated K_D were higher than 4.5. This means that they could be classified as liquefiable or non-liquefiable, according to the selected methodology.

Regarding the liquefaction analysis using methods based on the shear wave velocity, it was observed that according to the model of Kayen et al. (2013) the cyclic resistance was ranging between 0.10 and 0.20, in the range of the shear wave velocities of Puerto Baquerizo site. The estimated safety factors were in the order of 0.30 to 0.40, approximately. An important aspect that should be noted in the model of Kayen et al. (2013) is the relatively little influence of the fines content on the prediction of the cyclic resistance rate.

On the other hand, through Andrus and Stokoe (2000) cyclic resistances between 0.04 to 0.16 were determined for sands with fines contents less than 5%. Therefore, the estimated safety factors against liquefaction were between 0.30 and 0.50, magnitudes that are consistent with what was predicted by the other selected methodologies.

However, unlike what was observed in Kayen et al. (2013), the Andrus and Stokoe (2000) method includes a stronger influence of the fines content on the cyclic resistance ratio. Andrus and Stokoe (2000) detected three different CRR-V_S curves associated to percentages of fines contents for which the cyclic resistance can be defined as a function of the shear wave velocity: FC less than 5%, FC between 5% and 35%, and FC greater than 35%. This effect is more noticeable in the range between 160 m/s and 200 m/s, where the cyclic resistance ratio of a clean sand (fines content less than 5%) can be half of the cyclic resistance ratio of a sand with more than 35% fines (full black line and black dashed line in Fig. 4).

Another important point to note is that the methodology of Andrus and Stokoe (2000) was more conservative than Kayen et al. (2013) for shear wave velocities less than 150 m/s and 180 m/s, associated to clean sands and with fines content greater than 35%, respectively. However, this trend is reversed at corrected shear wave velocities greater than the described limits, and it is more noticeable in the estimation of the cyclic resistance of soils with significant fines contents.

Using as input the liquefaction safety factors determined, the liquefaction potential index LPI (Iwasaki et al. 1982) and the Ishihara-inspired liquefaction potential index LPI_{ish} (Maurer et al. 2015) were calculated.

The LPI calculated from the K_D-based methodologies were ranging between 10.2 to 17.1. According to this results Puerto Baquerizo has a high or very high liquefaction potential. This is consistent with the estimations through methodologies based on shear wave velocity, where LPI were determined between 17.25 and 18.25, a magnitude that also corresponds to a very high potential.

On the other hand, the LPI_{ish} (Maurer et al. 2015) includes within the liquefaction potential analysis the effect of the existence and thickness of non-liquefiable layers above the liquefiable material. In the case of Puerto Baquerizo, the thickness of the non-liquefiable layer is 2.6 m (thickness of shallow clay stratum). For the KD-based methods, LPI_{ish} were determined between 7.0 and 11.9, which corresponds to high liquefaction potentials. These results coincide with the LPI_{ish} determined from the Vs methods, which also indicate a high liquefaction potential.

Table 1 summarizes the results found in the evaluation of the liquefaction potential for Puerto Baquerizo using the Iwasaki et al. (1982) and Maurer et al. (2015) relationships. The liquefaction potential indices calculated using the methodology proposed by Maurer et al. (2015) are between 35% and 45% lower than those calculated using the Iwasaki et al. (1982) method. However, both liquefaction potential indices correlate with liquefaction expressions in Puerto Baquerizo after the Mw6.6 earthquake in Ecuador.

5. Conclusions

The results of liquefaction potential assessment using the data obtained by the seismic dilatometer test (SDMT) indicate that Puerto Baquerizo has a high to very high liquefaction potential. This classification is consistent with the liquefaction expression levels observed in Puerto Baquerizo after the Mw6.6 earthquake of 2023. According to the results obtained, it is deduced that the main source of the manifestations of liquefaction at surface is the "silty sand" layer between 2.6 m and 6.5 m deep. However, seismic-induced liquefaction may be also triggered in the thin intercalations layer of cohesionless soils between 6.5 m and 16.5 m.

The analysis of this case of study indicates that liquefaction evaluation using K_D-based methods predict adequately the liquefaction potential in Quaternary cohesionless soils of the Coastal area of Ecuador. A good correlation was found in the results of the liquefaction assessments using several K_D-based and V_S-based methods, both in factors of safety and in the liquefaction severity indices (i.e. Iwasaki et al. 1982, Maurer et al. 2015). Further investigations, by means of piezocone or standard penetration tests, is also desirable to complement this research.

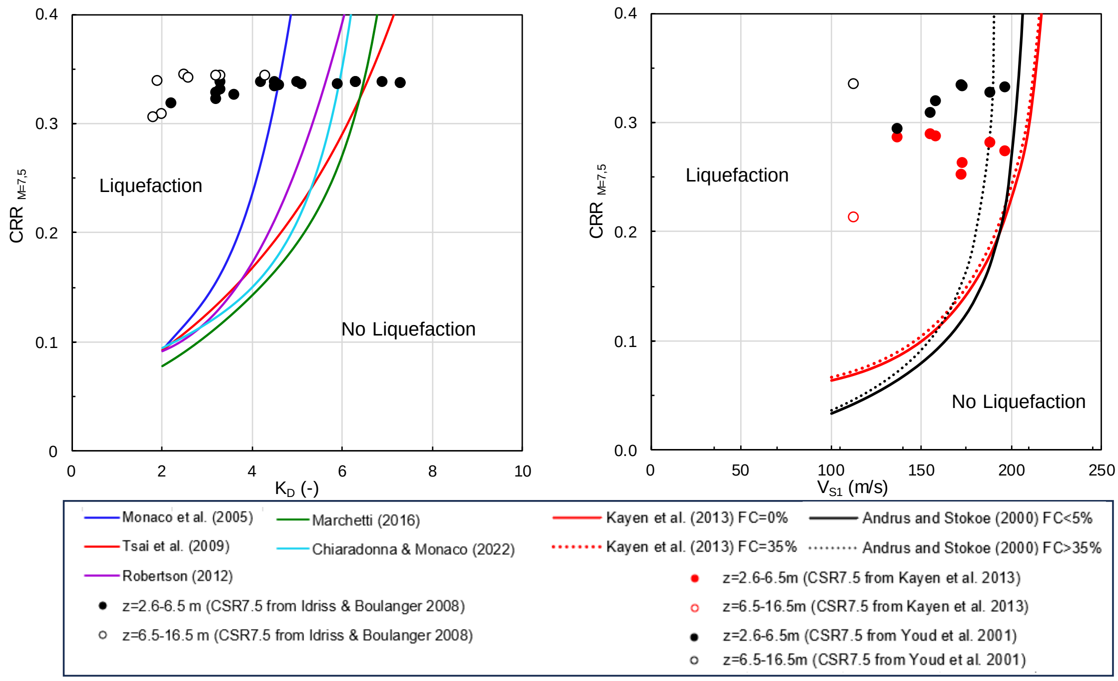

Figure 4. Cyclic resistance Ratio ($CRR_{7.5}$) curves for both K_D-based and Vs-based methods, and their relation with the predicted Cyclic stress ratio ($CSR_{7.5}$) in "silty sand" and "silty sand/ silty clay mixture" layers (data filtered for I_D>1.20 and FC>50%)

Table 1. Liquefaction Potential Index for Puerto Baquerizo estimated from SDMT test results

Method	**LPI (Iwasaki et al. 1982)**		**LPI_{ish} (Maurer et al. 2015)**	
	Magnitude	**Designation**	**Magnitude**	**Designation**
Monaco et al. (2005)	10.2	High	7.0	High
Tsai et al. (2009)	15.1	Very High	10.6	High
Robertson (2012)	14.1	High	9.8	High
Marchetti (2016)	17.1	Very High	11.9	High
Chiaradonna and Monaco (2022)	16.7	Very High	11.8	High
Andrus and Stokoe (2000)	17.2	Very High	13.0	High
Kayen et al. (2013)	18.2	Very High	14.2	High

Finally, the results of this work suggest that the use of the empirical relationships proposed by Di Buccio et al. (2023) between the Material Index (I_D) and the fines content (FC) allow estimate the cyclic resistance ratio ($CRR_{7.5}$) from the V_S-based on Andrus and Stokoe (2000) and Kayen et al. (2013) in the Coastal area of Ecuador, without the need of additional boreholes. However, further validation is recommended to study the applicability of this correlation in Ecuadorian soils, carrying out coupled boreholes and SDMTs.

References

Amoroso, S., Monaco, P., Rollins K. M., Holtrigter, M., and Thorp, A. "Liquefaction Assessment by Seismic Dilatometer Test (SDMT) after 2010-2011 Canterbury Earthquakes (New Zealand)." In: 6th International Conference on Earthquake Geotechnical Engineering, Christchurch, New Zealand, 2015.

Andrus, R., Stokoe, K. "Liquefaction Resistance of Soils from Shear-Wave Velocity", J. Geotech. Geoenvironmental Eng., 126 (11), pp. 1015-1025, 2000. https://doi.org/10.1061/(ASCE)1090-0241(2000)126:11(1015)

Atkinson, G. M., David, M. B. "Empirical Ground-Motion Relations for Subduction-Zone Earthquakes and Their Application to Cascadia and Other Regions", Bull. Seismol. Soc. Am., 93 (4), pp. 1703-1729, 2003. www.seismosoc.org.

Atkinson, G. M., David, M. B. "Earthquake Ground-Motion Prediction Equations for Eastern North America", Bull. Seismol. Soc. Am., 96 (6), pp. 2181–2205, 2006. https://doi.org/10.1785/0120050245.

Ballegooy, S. Van, P. Malan, V. Lacrosse, M. E. Jacka, M. Cubrinovski, J. D. Bray, T. D. O'Rourke, S. A. Crawford, and H. Cowan. "Assessment of Liquefaction-Induced Land Damage for Residential Christchurch", Earthquake Spectra 30 (1), 31–55, 2014. https://doi.org/10.1193/031813EQS070M.

Boulanger, R., and Idriss, I. "CPT and SPT Based Liquefaction Triggering Procedures", Center of Geotechnical Modeling. Department of Civil and Environmental Engineering, Davis, California, Report. UCD/CGM-14/01, 2014.

Di Buccio, F., Cesare, C., Fontana, D., Minarelli L., Vagnon, F., and Amoroso, S. "Fines Content Determination through Geotechnical and Geophysical Tests for Liquefaction Assessment in the Emilia Alluvial Plain (Ferrara, Italy)", Soil Dynamics and Earthquake Engineering, 173 (9), 2023. https://doi.org/10.1016/j.soildyn.2023.108057.

Cetin, K., Seed, R., Der Kiureghian, A., Tokimatsu, K., Harder, L., Kayen, R., and Moss, R. "Standard Penetration Test-Based Probabilistic and Deterministic Assessment of Seismic Soil Liquefaction Potential", J. of Geotechnical and Geoenvironmental Engineering, 130 (12), 1314-1340, 2004. https://doi.org/10.1061/(ASCE)1090-0241(2004)130:12(1314)

Chiaradonna, A., and Monaco, P. "Assessment of Liquefaction Triggering by Seismic Dilatometer Tests: Comparison between Semi-Empirical Approchaes and Non-Linear Dynamic Analyses", In: 20th International Conference on Soil Mechanics and Geoetechnical Engineering, Australia. 2022.

Eguez, A., Gaona, M., and Albán, A. "Geological Map of the Republic of Ecuador", National Institute for Geological, Mining and Metallurgical Research. 2017. https://www.geoenergia.gob.ec/mapas-geologicos/.

Idriss, I., and Boulanger, R., "Soil Liquefaction during Earthquakes", 1st ed. EERI, Oakland. 2008.

Ishihara, K. "Stability of Natural Deposits during Earthquakes", In: 11th International Conference on Soil Mechanics and Foundation Engineering, San Francisco, 1985.

Kavazanjian, E., Andrade, J., Arul Arulmoli, K., Atwater, B., Christian, J., Green, R., Kramer, S., et al. "State of the Art and Practice in the Assessment of Earthquake-Induced Soil Liquefaction and Its Consequences", National Academies Press, Washington, 2022. https://doi.org/10.17226/23474.

Kayen, R., Moss, R., Thompson, E., Seed, R., Cetin, K., Der Kiureghian, A., Tanaka, Y., and Tokimatsu, K. "Shear-Wave Velocity-Based Probabilistic and Deterministic Assessment of Seismic Soil Liquefaction Potencial", Journal of Geotechnical and Geoenvironmental Engineering (139), pp. 407-419, 2013.

Kishida T., and Tsai, C. "Damage to Reinforced Concrete Buildings in Niigata City with Special Reference to Foundation Engineering". Soils and Foundations, 6(1), pp. 71-88, 1966. https://doi.org/10.3208/sandf1960.6.71

Marchetti, S., Crapps, D. K. "Flat Dilatometer Manual", G.P.E. Inc, Italy, 1981

Marchetti, S. "Detection of Liquefiable Sand Layers by Means of Quasi Static Penetration Tests", In: 2nd European Symp. on Penetration Testing. Netherlands, 1982.

Marchetti, S., Monaco, P., Totani G., and Marchetti D. "In Situ Tests by Seismic Dilatometer (SDMT)", American Society of Civil Engineers (ASCE), 292–311, 2008. https://doi.org/10.1061/40962(325)7.

Marchetti, S. "Incorporating the Stress History Parameter KD of DMT into the Liquefaction Correlations in Clean Uncemented Sands", Journal of Geotechnical and Geoenvironmental Engineering 142 (2), 2016. https://doi.org/10.1061/(asce)gt.1943-5606.0001380.

Maurer, B. W., Green, R. A., and Taylor, O. "Moving towards an Improved Index for Assessing Liquefaction Hazard: Lessons from Historical Data", Soils and Foundations, 55 (4): 778–87, 2015. https://doi.org/10.1016/j.sandf.2015.06.010. OJO

Monaco, P., and Amoroso, S. "Review of the Liquefaction Cases Triggered by the 2009 L'Aquila Earthquake (Italy)", Earthquake Geotechnical Engineering for Protection and Development of Environment and Constructions, Italy, 2019.

Monaco, P, Marchetti, S., Totani, G., and Calabrese, M. "Sand Liquefiability Assessment by Flat Dilatometer Test (DMT)", In: 16th Int. Conf. on Soil Mechanics and Geotechnical Engineering, Japan, 2005.

Monaco, P., Santucci, F., Grasso, S., Marchetti, S., Maugeri, M., and Totani, G. "Analysis of the Liquefaction Phenomena in the Village of Vittorito (L'Aquila)", In: Bulletin of Earthquake Engineering 9 (1), 231–61, 2011. https://doi.org/10.1007/s10518-010-9228-0. OJO

Moss, R., Seed, R., Kayen, R., Stewart, J., Der Kiureghian, A., and Cetin, K. "CPT-Based Probabilistic and Deterministic Assessment of in Situ Seismic Soil Liquefaction Potential", Journal of Geotechnical and Geoenvironmental Engineering, 132(8), pp., 1032-1051, 2006. https://doi.org/10.1061/(ASCE)1090-0241(2006)132:8(1032)

Ortiz-Hernández, E., Chunga, K., Toulkeridis, T., and Pastor J. L. "Soil Liquefaction and Other Seismic-Associated Phenomena in the City of Chone during the 2016 Earthquake of Coastal Ecuador", Applied Sciences (Switzerland), 12 (15), 7867, 2022. https://doi.org/10.3390/app12157867.

Reyna, F., and Chameau, J. "Dilatometer Based Liquefaction Potential of Sites in the Imperial Valley", In: 2nd International Conference on Recent Advances in Geotechnical, Missouri, 1991.

Robertson, P. "Interpretation of In-Situ Tests- Some Insights", In: 4th International Conference on Site Characterization, Netherlands, 2012.

Robertson, P., and Campanella, R. "Estimating Liquefaction Potential of Sands Using the Plate Dilatometer", Geotechnical Testing Jorunal., 9 (1), 1986.

Salocchi, A. C., Minarelli L., Lugli, S., Amoroso S.,. Rollins, K. M., and Fontana D., "Liquefaction Source Layer for Sand Blows Induced by the 2016 Megathrust Earthquake (Mw 7.8) in Ecuador (Boca de Briceño)", Journal of South American Earth Sciences 103, 2020. https://doi.org/10.1016/j.jsames.2020.102737.

Seed, H., and Idriss, I. "Simplified Procedure for Evaluating Soil Liquefaction Potential", Journal of Soil Mechanics and Foundation Engineering, 97 (9), pp., 1249-1273, 1971. https://doi.org/10.1061/JSFEAQ.0001662.

Tsai, P. Lee, H., Kung, G. T., and Juang, C. H. "Simplified DMT-Based Methods for Evaluating Liquefaction Resistance of Soils", Engineering Geology 103 (1–2), pp., 13–22, 2009. https://doi.org/10.1016/j.enggeo.2008.07.008.

Vera Grunauer, X., Lopez-Zhindon, S., Ordoñez J., and Chavez M. "Liquefaction Case Histories after the 2016 Megathrust Pedernales Earthquake in Ecuador", Earthquake Geotechnical Engineering for Protection and Development of Environmental and Constructions, Italy, 2019. https://www.researchgate.net/publication/341090265.

Yu., H. "James K. Mitchell Lecture. In Situ Soil Testing: From Mechanics to Interpretation", In: ISC-2 on Geothecnical and Geophysical Site Characterization, pp. 165-195, Portugal, 2004.

Youd, T., Idriss, I., Andrus, R., Arango, I., Castro G., Christian, J., Dobry, R., et al. "Liquefaction Resistance of Soil: Summary Report from the 1996 NCEER and 1998 NCEER/NSF Workshops on Evaluation of Liquefaction Resistance of Soils", Journal of Geotechnical and Geoenvironmental Engineering, 127 (10), pp., 817-833, 2001

Youngs, R., Chiou, W., Silva J., and Humphrey, J. "Strong Ground Motion Attenuation Relationships for Subduction Zone Earthquakes", Seismological Research Letters 68 (1), pp., 58–73, 1997. https://doi.org/10.1785/gssrl.68.1.58.

Zhao, J., Zhang, J., Akihiro, A., Ohno, Y., Oouchi, T., Takahashi, T., Hiroshi, O., et al. "Attenuation Relations of Strong Ground Motion in Japan Using Site Classification Based on Predominant Period", Bulletin of the Seismological Society of America, 96 (3), pp. 898-913, 2006. https://doi.org/10.1785/0120050122.

Zhou, S. "Evaluation of the Liquefaction of Sand by Static Cone Penetration Test", In: 7th World Conference on Earthqueake Engineering, Turkey, 1980.